

## Corrosion Inhibition of Aluminum by Using Synthesized Dipyrindinium Salts

A.A.Ganash\*, A.Y.Obaid, Shabaan A.K.Elroby, Abou-Elhagag A. Hermas

Chemistry Department, Faculty of Science, King Abdulaziz University, Jeddah 21589, Saudi Arabia

\*E-mail: [aganash@kau.edu.sa](mailto:aganash@kau.edu.sa)

*Received:* 6 April 2016 / *Accepted:* 21 May 2016 / *Published:* 4 June 2016

---

Some synthesized bipyridinium rings-containing compounds have been used as inhibitors of corrosion of aluminum in 1 M HCl at 45°C. Three dipyrindinium compounds, DMdPyI, HMdPyBr and BMPyEI, and mono-pyridinium ring compound, TMPyI, were studied. Corrosion potential-time, cathodic-anodic polarization and impedance electrochemical measurements, and quantum calculations were applied. The study indicated that these compounds work as anodic inhibitors for Al, except higher concentrations of HMdPyBr and BMPyEI has additionally some cathodic inhibitive action. The inhibition efficiency of these compounds increased with increasing the inhibitor concentration reaching a plateau at  $1 \times 10^{-4}$  M and the highest inhibition was observed by the compound BMPyEI. The inhibitors follow Langmuir adsorption isotherm, and the adsorption is endothermic and increase with temperature. The inhibitor compounds are adsorbed mainly physically and spontaneously on the aluminum surface.

---

**Keywords:** Corrosion protection, Aluminum, Dipyrindinium Salts, inhibitors

### 1. INTRODUCTION

Aluminum and its alloys are important materials due to their wide applications in industrial and technological works, like automobile, aerospace, household industries and in marine and other applications [1–3]. But, they are reactive materials and are exposed to corrosion. Various attempts have been made to study the influence of different ions on the electrochemical behavior and pitting corrosion of Al and its alloys [4–6], and also the research in Al electrochemical behavior and corrosion inhibition in wide variety of media [7].

Corrosion inhibitors are widely used in industry. Development of new materials as inhibitors is required to meet the increased demands of corrosion inhibition. Adsorption of the inhibitors onto the metal surface is an essential step in the inhibition process. It is influenced by the nature and surface

charge of the metal, by the chemical structure of the organic inhibitor, and by the type of aggressive electrolyte. Physical (electrostatic) adsorption and chemisorption are the principal types of interaction between an organic inhibitor and metal surface. The electrical characteristic of the organic inhibitors is significant in the adsorption of these inhibitors. Most organic inhibitors are substances with at least one functional group regarded as the reaction center for the chemisorption process. In this case the strength of the adsorption bond is related to the heteroatom electron density and to the function group polarizability.

Quaternary pyridinium compounds are a type of cationic organic corrosion inhibitor used for the protection of metals [8–10]. Wang et al showed that cetyl pyridinium chloride is effective for the inhibition of C-steel over a wide concentration range of aqueous solution of phosphoric acid [15]. Abd El-Maksoud studied the inhibition of both iron and copper in HCl and H<sub>2</sub>SO<sub>4</sub> by hexadecyl pyridinium bromide [10]. Viologens (*N,N*-diquaternized bipyridinium salts) are found as an effective inhibitor of zinc in HCl and carbon steel in H<sub>2</sub>SO<sub>4</sub> [11]. Viologens are used in a variety of other studies, including electron transfer mediation to various biological molecules, the surface enhanced Raman studies of the adsorption at electrode surfaces, the behavior of supramolecular assemblies at electrode surfaces and the applications for the electrochromic display devices [12]. In this paper some synthesized *N,N*-diquaternized bipyridinium salts with different structures are used as inhibitors of pure aluminum in concentrated hydrochloric acid solution.

## 2. EXPERIMENTAL

### 2.1. Inhibitor preparation

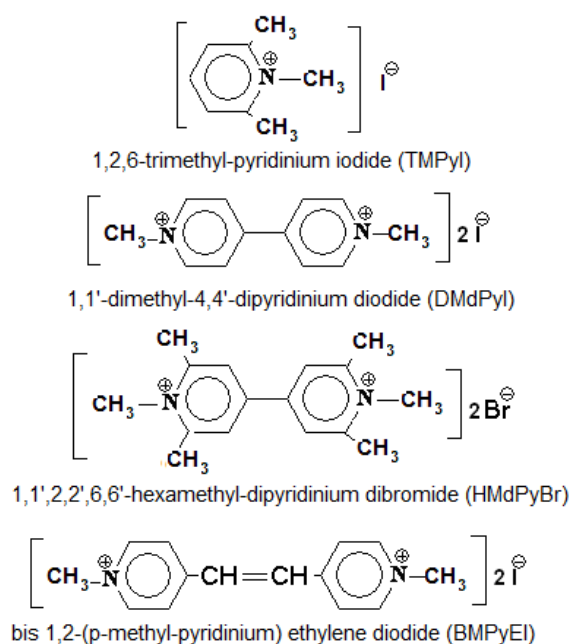


**Figure 1.** Chemical structures of the inhibitor compounds.

The bipyridines compounds, the structures are indicated in Fig.1, used in this study were prepared as described before [11,13] and the chemical composition were examined by melting point measurement, elemental analysis and  $^1\text{H}$ NMR analysis.

## 2.2. Electrochemical Corrosion test

An electrochemical cell with a three-electrode was used for electrochemical measurements; aluminum rod (1 cm in diameter) coated with epoxy leaving the bottom working area of  $0.79\text{ cm}^2$ , a platinum sheet, and a Metrohm Ag/AgCl electrode (in 3 M KCl) were used as working, counter and reference electrodes, respectively. Potentiodynamic polarization and electrochemical impedance spectroscopy (EIS) measurement were carried out in different temperatures and range of inhibitor concentration using a potentiostat of type Autolab PGSTAT30, coupled to a computer equipped with GPES software for potential and polarization measurements and FRA software for EIS measurement.

The polarization curves were recorded with a scan rate of  $0.001\text{ V s}^{-1}$ , where the initial potential was the corrosion potential value reached after short time (about 15 minutes) of exposure. The polarization curves were obtained starting from the open circuit potential (OCP) and varying the potential up to 200 mV in anodic branch and down to  $-200\text{ mV}$  cathodic branch of the Tafel plot. Electrochemical impedance spectroscopy data were obtained at OCP over a frequency range from 50 kHz to 0.1 Hz using AC amplitude of 10 mV.

## 2.3. Computational Details

In the computational section, the molecular structures of the studied compounds were geometrically optimized using the Density Functional Theory (DFT) method with B3LYP/6-311+G\*\* level of theory. The DFT has been used to describe the mechanism of an interaction between inhibitor and surface of metal in corrosion studies [14–17]. All calculations were carried out using Gaussian 09W [29]. B3LYP, a version of the DFT method that uses Becke's three parameter functional (B3) and includes a mixture of HF with DFT exchange terms associated with the gradient corrected correlation functional of Lee, Yang and Parr (LYP) [18], was used in this paper to carry out quantum calculations.

# 3. RESULTS AND DISCUSSION

## 3.1. Corrosion potential – time behavior

The change of corrosion potential,  $E_{\text{cor}}$ , with time is important technique to recognize the corrosion behavior of the metal and the effect of inhibitors. Figure 2 describe variation of  $E_{\text{cor}}$  of aluminum metal with time in aerated solution of 1M HCl at  $45^\circ\text{C}$  in presences and absence of different concentration of the inhibitor. The potential in the uninhibited solution stabilized after a period of time ( $\sim 1000$  seconds) when it became between  $-950$  and  $-975\text{ mV}$  (Ag/AgCl). While the addition of inhibitor shift the potential to anodic region (positive direction) and the effect increase with increasing

of inhibitor concentration as shown in Fig.2-A for TMPyI and Fig.2-B for HMdPyBr. The potential-time curves in presence of different concentrations of DMdPyI are similar to those of HMdPyBr (Fig.2-B). In case of BMPyEI (Fig.2-C), the lowest concentration ( $1 \times 10^{-5}$ ) shifted  $E_{\text{cor}}$  to cathodic region (negative direction), while the higher concentrations of the inhibitor shifted  $E_{\text{cor}}$  to anodic direction. These results released the bipyridinium compounds inhibit the anodic reaction (metal dissolution) more than the cathodic reaction on the metal surface. Similar behavior for these compounds was obtained when worked as inhibitors for corrosion of stainless steel in hydrochloric acid solution[13].

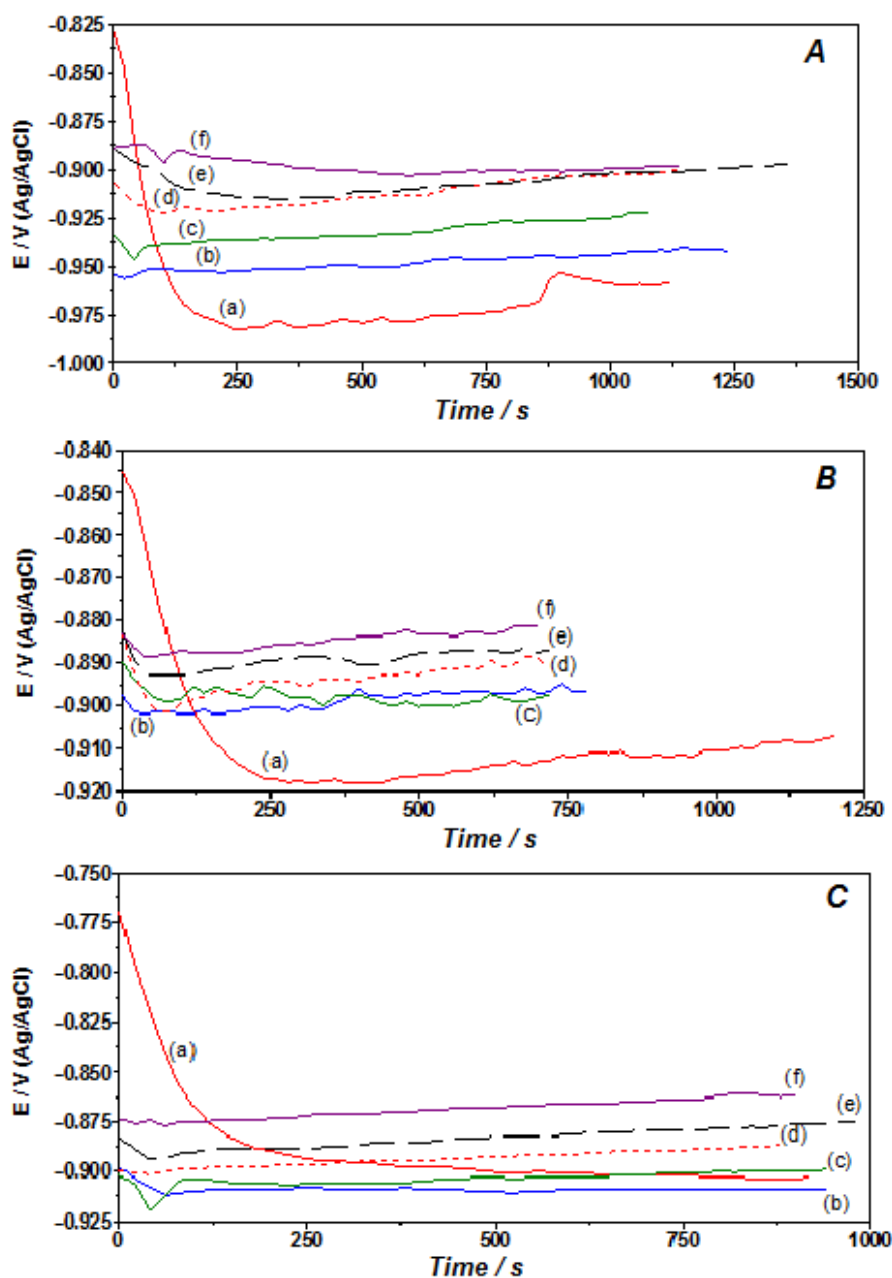


**Figure 2.** Effect of addition of Inhibitors TMPyI (A), HMdPyBr (B) and BMdPyEI (C) at different concentrations; (a) pure solution, (b)  $1 \times 10^{-5}$  M, (c)  $5 \times 10^{-5}$  M, (d)  $1 \times 10^{-4}$  M, (e)  $5 \times 10^{-4}$  M and (f)  $1 \times 10^{-3}$  M on corrosion potential of aluminum in 1M HCl at 45°C.

3.2. Cathodic-anodic polarization

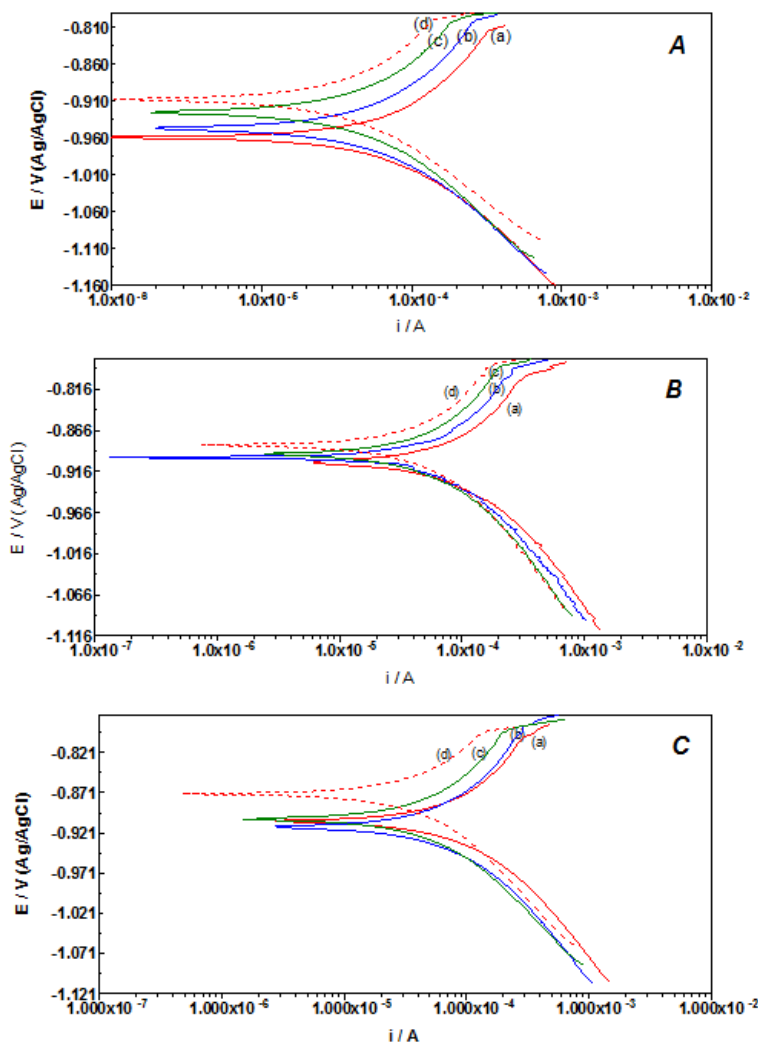


**Figure 3.** The cathodic-anodic polarization of aluminum in 1M HCl at 45°C in absence and presence of inhibitors TMPyI (A), HMdPyBr (B) and BMdPyEI (C) at different concentrations; (a) pure solution, (b) 1x10<sup>-5</sup> M, (c) 1x10<sup>-4</sup> M, (d) 1x10<sup>-3</sup> M.

Figure 3 show the cathodic - anodic polarization curves (Tafel plots) for aluminum electrode in 1M HCl in presence and absences of different concentrations of inhibitor at 45°C. The cathodic and anodic Tafel lines were determined and used to estimate the corrosion parameters which are tabulated in Table (1), the inhibition efficiency was calculated using the following equation:

$$IE = \frac{i_{cor}^{\circ} - i_{cor}}{i_{cor}^{\circ}} \times 100 \quad (1)$$

Where, the  $i_{cor}^{\circ}$  and  $i_{cor}$  are the corrosion current of Al in uninhibited and inhibited solutions. Figure 3-A shows the polarization curves in absence and presence of different concentrations of the mono-pyridinium salt TMPyI. The anodic branch shifted in parallel behavior to lower current densities with increasing of inhibitor concentration, indicating of the inhibitive action of this compound to the

anodic reaction, while no effect on the cathodic curve or cathodic reaction with exception of the highest concentration that increased the cathodic current significantly. Nevertheless, the highest value is about 55% inhibition at the highest concentration of the inhibitor.

Figure 3-B and Figure 3-C indicates the polarization behaviors in presence of the dipyridinium salts HMdPyBr and BMPyEI, respectively, the two compounds as well the third one DMdPyI (its curves not shown here) reduced both the anodic and cathodic current but the inhibitive effect still larger on the anode reaction. These compounds could be defined as mixed inhibitor with mainly anodic. The inhibition was generally the highest in the case of BMPyEI, reaching the highest rate for 57% inhibition at the largest concentration. The Tafel and corrosion parameters of Al in presence of the four studied inhibitors are included in Table 1.

**Table 1.** Cathodic-anodic polarization parameters of Al in absence and presence of different inhibitor concentrations in 1 M HCl at 45°C

Inhibit	Concn. (M)	$-E_{cor}$ (mV)	$I_{cor}$ ( $\mu A.cm^{-2}$ )	$B_c$ (mV/decade)	$B_a$	IE (%)
TMPyI	Pure	959	133	171	184	
	$1 \times 10^{-5}$	947	106.4	178	182	20.0
	$5 \times 10^{-5}$	924	87.0	181	175	35.5
	$1 \times 10^{-4}$	905	66.23	175	152	50.2
	$5 \times 10^{-4}$	903	65.2	164	158	51.0
	$1 \times 10^{-3}$	907	65.8	150	174	55.5
DMdP	Pure	929	126	150	171	
	$1 \times 10^{-5}$	925	109.6	154	180	13.0
	$5 \times 10^{-5}$	921	99.5	163	158	21.0
	$1 \times 10^{-4}$	919	90.1	154	170	28.5
	$5 \times 10^{-4}$	910	73.6	174	151	41.6
	$1 \times 10^{-3}$	895	70.3	174	156	44.2
HMdP	Pure	910	110	157	145	
	$1 \times 10^{-5}$	902	90.2	165	170	18.0
	$5 \times 10^{-5}$	903	85.0	175	176	23.0
	$1 \times 10^{-4}$	895	70.4	173	159	36.0
	$5 \times 10^{-4}$	893	66.6	172	167	39.5
	$1 \times 10^{-3}$	884	62.7	183	157	43.2
BMPy	Pure	907	136	152	159	
	$1 \times 10^{-5}$	914	116.1	170	174	14.6
	$5 \times 10^{-5}$	912	92.9	154	174	31.7
	$1 \times 10^{-4}$	905	76.6	147	158	43.7
	$5 \times 10^{-4}$	892	66	150	141	51.5
	$1 \times 10^{-3}$	873	57.8	154	110	57.5

The results in Table 1 indicate that the four studied inhibitors show analogous behavior as the inhibition efficiency increased with increasing concentration and reached to like a plateau IE value at inhibitor concentration  $1 \times 10^{-4} M$ . This behavior is characteristic of these studied compounds; similar results were obtained with steel in sulfuric acid [11] and stainless steel in hydrochloric acid [13], and

other surfactants in hydrochloric acid [19]. The calculated anodic and cathodic Tafel slopes  $B_a$  and  $B_c$  respectively, in Table 1 are higher than the theoretical values for active metals in an acid solution, but they are consistent with the values of the aluminum metal, this is due to presence of the surface oxide which raises the values of Tafel slope. The presence of the inhibitor did not change the values of  $B_a$  and  $B_c$  which indicates no change in mechanism of cathodic and anodic reaction on the aluminum surface.

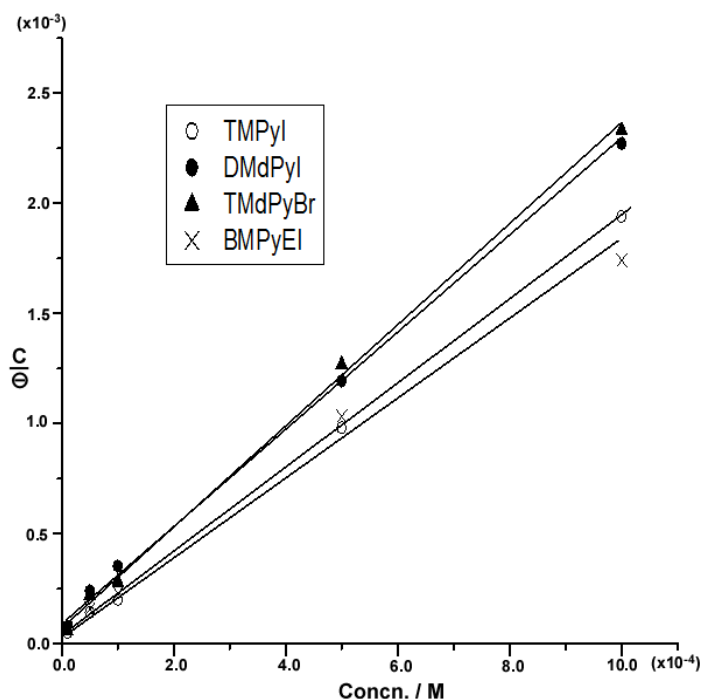


**Figure 4.** Langmuir adsorption isotherm of the different inhibitors inhibitor on Al in 1M HCl at 45°C.

The organic compound works as corrosion inhibitor through adsorption on the metal surface. The degree of adsorption inhibitor ( $\theta$ ) on the electrode surface can be calculated from the equation:

$$\theta = 1 - \frac{i_{cor}}{i_{cor}^{\circ}} \quad (2)$$

By plotting  $C/\theta$  versus inhibitor concentration ( $C$ ) fit a straight line as represented by the data of BMPyEI in Fig.5. The adsorptions of the compounds under study agree with the Langmuir adsorption isotherm [20][32], it is possible to use the equation:

$$\frac{C}{\theta} = \frac{1}{K} + C \quad (3)$$

Where,  $K$  is the equilibrium constant for the adsorption process.

The relationship between  $K$  and the free energy of adsorption ( $\Delta G_{ads}^{\circ}$ ) can be deduced from the equation:

$$K = \frac{1}{55.5} \exp\left(\frac{-\Delta G_{ads}^\circ}{RT}\right) \quad (4)$$

Where R is the gases constant and T is the absolute temperature, the free energy of adsorption inhibitors under study on the aluminum surface was calculated and the results recorded in Table (2). The values of  $\Delta G_{ads}^\circ$  of the studied inhibitors in Al/HCl solution are close to those in the stainless steel/HCl solution [13]. These values (less than 20 KJ/mol) are characteristic of physical adsorption and its negative mean that the adsorption of these compounds on the aluminum surface is a spontaneous process. In addition the higher values of equilibrium constant indicate strong adsorption process.

**Table 2.** Adsorption isotherm parameters of the studies inhibitors on Al in 1 M HCl at at 45°C

Inhibitor	Slope	K	- $\Delta G^\circ$ (kJ mol <sup>-1</sup> )
TMPyI	1.93	4.0x10 <sup>4</sup>	19.7
DMdPyI	2.17	9.4x10 <sup>3</sup>	13.6
HMdPyBr	2.26	1.34x10 <sup>4</sup>	14.6
BMPyEI	1.7	1.47x10 <sup>4</sup>	14.8

### 3.3 Electrochemical impedance spectroscopy study

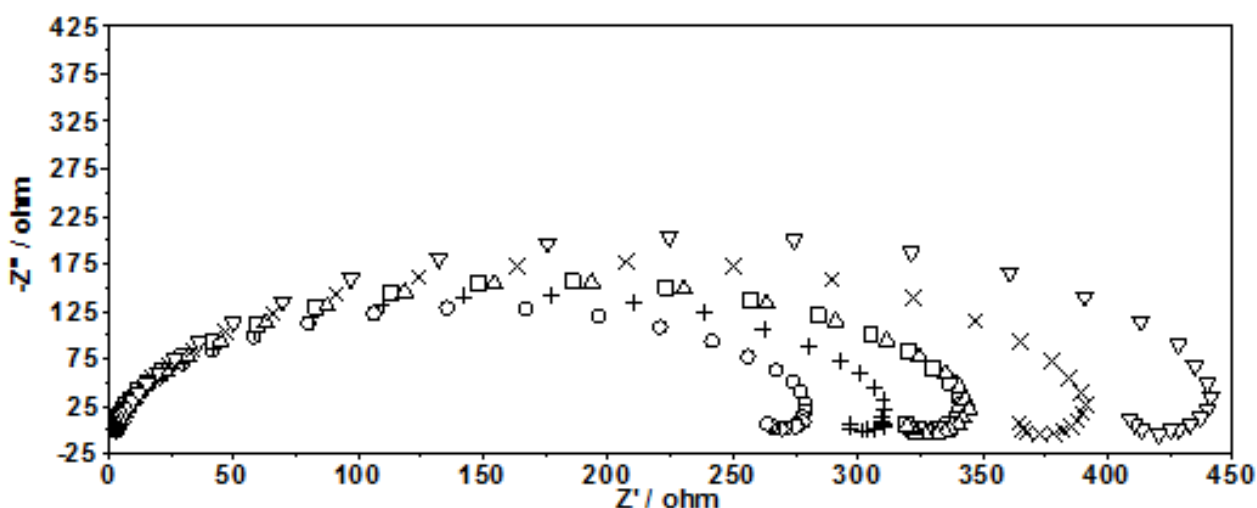


**Figure 5.** EIS spectra of Al in 1 M HCl at 45°C (○) and in presence of 1x10<sup>-5</sup> M (+), 5x10<sup>-5</sup> M (□), 1x10<sup>-4</sup> M (Δ), 5x10<sup>-4</sup> M (x) and 1x10<sup>-3</sup> M (▽) BMdPyEI.

The electrochemical impedance spectroscopy (EIS) was measured at open circuit potential of aluminum in 1M HCl in absence and presence of the inhibitor at 45°C.

Fig.5 represents the Nequist plots in presence of different concentrations of BMPyEI inhibitor, the plot shows large semi-circle with capacitive loop at high frequency region and small inductive loop at low frequency region. The semi circuit describes the resistance of charge transfer through the corrosion process; in the other side, the inductive loop represents the adsorption process of hydrogen ions and inhibitor molecules [21]. As shown from the figure, the addition of inhibitors did not change the curve shape and have no effect other than increase the diameter of circuit with increasing of inhibitor concentration, this strong evidence of increase of inhibition efficiency.

The measurement revealed that the corrosion process of aluminum electrode in HCl is under charge transfer control, this process was fitted with the equivalent circuit  $R_s(R_p Q_{dl}$  (Fig. 6), where  $R_s$  represents the solution resistance,  $R_p$  is charge transfer resistance and  $C_{dl}$  (or  $Q_{dl}$  a constant phase element) is capacity of the electrical double layer. The EIS parameters were calculated, as recorded in Table (3), and the  $R_p$  values were used to calculate the inhibition efficiency as in following equation:

$$IE = \frac{R_p - R_p^\circ}{R_p} \times 100 \quad (5)$$

and  $R_p$  and  $R_p^\circ$  are the charge transfer resistance of uninhibited and inhibited solution respectively. The analysis of EIS data indicates that all the compounds inhibited the corrosion of Al in the concentrated HCl and the inhibition efficiency increased with concentration. The two compounds HMdPyBr and BMPyEI exhibited the highest inhibition efficiency in comparison with the other compounds.

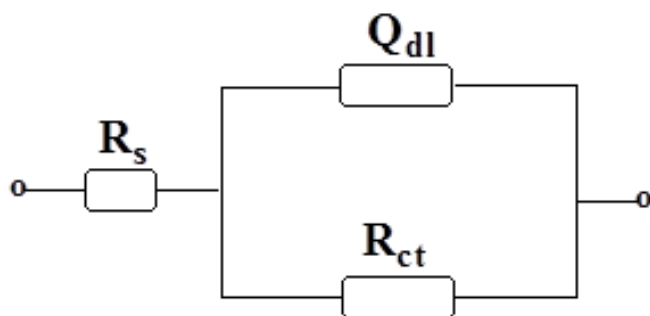


Figure 6. The equivalent circuit used for the measured EIS.

Table 3. EIS parameters of Al in absence and presence of different inhibitor concentrations in 1 M HCl at 45°C

Inhibitor	Concn. (M)	$R_s$ ( $\Omega$ )	$R_p$ ( $\Omega$ )	$Q_{dl}$ (F)	n	IE (%)
TMPyI	Pure	2.8	345	$5.67 \times 10^{-5}$	0.93	
	$1 \times 10^{-5}$	2.7	390	$5.11 \times 10^{-5}$	0.93	11.6
	$5 \times 10^{-5}$	3.0	403	$4.92 \times 10^{-5}$	0.93	14.5
	$1 \times 10^{-4}$	2.9	415	$4.53 \times 10^{-5}$	0.94	17.0

	5x10 <sup>-4</sup>	3.2	438	4.25x10 <sup>-5</sup>	0.94	21.5
	1x10 <sup>-3</sup>	3.2	481	4.04x10 <sup>-5</sup>	0.94	28.8
DMdPyI	Pure	2.7	302	4.13x10 <sup>-5</sup>	0.95	
	1x10 <sup>-5</sup>	1.8	325	4.0x10 <sup>-5</sup>	0.95	7.2
	5x10 <sup>-5</sup>	1.8	338	3.83x10 <sup>-5</sup>	0.95	10.7
	1x10 <sup>-4</sup>	3.7	345	4.37x10 <sup>-5</sup>	0.95	12.5
	5x10 <sup>-4</sup>	1.9	365	4.1x10 <sup>-5</sup>	0.95	17.5
	1x10 <sup>-3</sup>	1.6	440	4.13x10 <sup>-5</sup>	0.82	31.4
HMdPyBr	Pure	2.2	340	6.52x10 <sup>-5</sup>	0.93	
	1x10 <sup>-5</sup>	2.8	460	5.8x10 <sup>-5</sup>	0.93	26.2
	5x10 <sup>-5</sup>	3.0	515	5.5x10 <sup>-5</sup>	0.94	33.7
	1x10 <sup>-4</sup>	3.2	545	5.1x10 <sup>-5</sup>	0.95	37.3
	5x10 <sup>-4</sup>	2.8	560	5.1x10 <sup>-5</sup>	0.95	39.5
	1x10 <sup>-3</sup>	2.8	573	5.1x10 <sup>-5</sup>	0.82	41.4
BMPyEI	Pure	2.0	280	5.5x10 <sup>-5</sup>	0.93	
	1x10 <sup>-5</sup>	2.1	325	5.0x10 <sup>-5</sup>	0.94	14.0
	5x10 <sup>-5</sup>	2.2	354	5.0x10 <sup>-5</sup>	0.94	21.0
	1x10 <sup>-4</sup>	2.2	364	4.7x10 <sup>-5</sup>	0.95	23.1
	5x10 <sup>-4</sup>	2.3	405	5.1x10 <sup>-5</sup>	0.95	30.9
	1x10 <sup>-3</sup>	3.0	457	4.1x10 <sup>-5</sup>	0.94	38.7

### 3.4. Effect of temperature

The effects of temperature (30-50°C) on the corrosion and polarization behavior of Al in 1M hydrochloric acid and in the presence of 5x10<sup>-4</sup> M inhibitor compound were studied; the values of cathodic-anodic polarization parameters were calculated and recorded in the Table (4). Although the corrosion current increased with increasing temperature the inhibition efficiency of the studied inhibitors increased. Previously, these compounds exhibited similar inhibition action for corrosion of stainless steel [22] and mild steel [18] in acidic solutions.

From Arrhenius equation:

$$\log i_{cor} = \log \lambda - \frac{E_a}{2.303 RT} \quad (6)$$

Where  $\lambda$  is the exponential factor and  $E_a$  is the activation energy of corrosion. A straight line could be obtained by plotting  $\log i_{cor}$  against  $1/T$  as shown in Fig.7 for Al in pure solution and in presence of inhibitor (two inhibitors were only represented). The activation energy was calculated and recorded in Table (5). The heat of inhibitor adsorption ( $\Delta H^\circ$ ) was calculated graphically from the following Langmuir adsorption equation:

$$\log \left( \frac{\theta}{1-\theta} \right) = \log A + \log C - \frac{\Delta H^\circ}{2.303 RT} \quad (7)$$

Where A is a constant does not depend on temperature. The values of  $\Delta H^\circ$  for adsorption of the studied inhibitors on Al electrode in 1M HCl are recorded in Table (5). Positive values for the heat of adsorption indicate that the process of adsorption is endothermic; therefore, inhibition efficiency increases with temperature. The BMPyEI compound exhibited the highest adsorption energy.

Moreover, the estimated values of  $E_a$  indicate significant decrease of the activation energy of corrosion process in presence of the inhibitors under study and the inhibitor BMPyI caused the lowest  $E_a$  values. The decrease in the activation energy in presence of the inhibitor indicates the chemical adsorption process of the inhibitor molecule on the surface of Al.

Although the values of  $\Delta G_{ads}^\circ$  of the studied inhibitors, as shown above, indicate physical adsorption process of the inhibitor molecule, the values of  $E_a$  indicate the chemical adsorption process. This means that the adsorption process of the inhibitors under study involve both the physical as well as the chemical adsorption.

**Table 4.** Cathodic-anodic polarization parameters of Al in 1 M HCl and in presence of  $5 \times 10^{-4}$  M inhibitor at different temperatures

Inhibitor	Temp. (°C)	$-E_{cor}$ (mV)	$I_{cor}$ ( $\mu A \cdot cm^{-2}$ )	$B_c$ (mV/decade)	$B_a$ (mV/decade)	IE (%)
Pure	30	905	79.4	143	164	
	35	906	97.2	154	163	
	40	912	123.5	155	176	
	45	918	119.5	172	167	
	50	920	166.9	159	187	
TMPyI	30	891	39.5	150	171	50
	35	898	45.7	148	163	53.0
	40	896	57.0	144	142	53.8
	45	903	55.0	164	158	54.0
	50	905	67.5	145	139	59.6
DMdPyI	30	886	26.7	165	149	39.5
	35	894	33.8	159	158	42.9
	40	898	40.8	153	169	45.8
	45	905	58.0	154	181	51.3
	50	911	70.2	160	196	53.6
HMdPyBr	30	873	49.2	150	152	38
	35	879	55.5	154	165	42.9
	40	895	60.3	144	157	51.2
	45	893	65.5	149	171	45.2
	50	914	76.1	141	163	54.4
BMPyEI	30	876	43.5	151	123	45.2
	35	884	47.8	148	157	50.8
	40	892	52.5	162	167	45.5
	45	910	55.0	174	151	59.4
	50	880	57.2	149	113	65.7

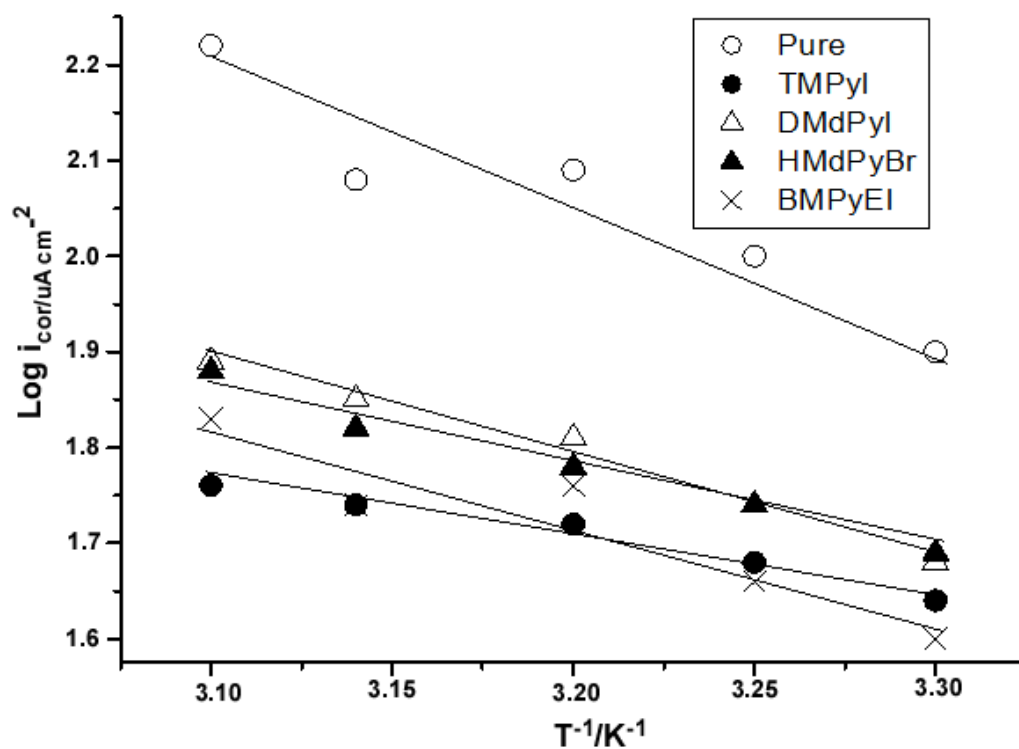


Figure 7. Arrhenius plots for the corrosion of the aluminum in 1 M HCl and in presence of inhibitors.

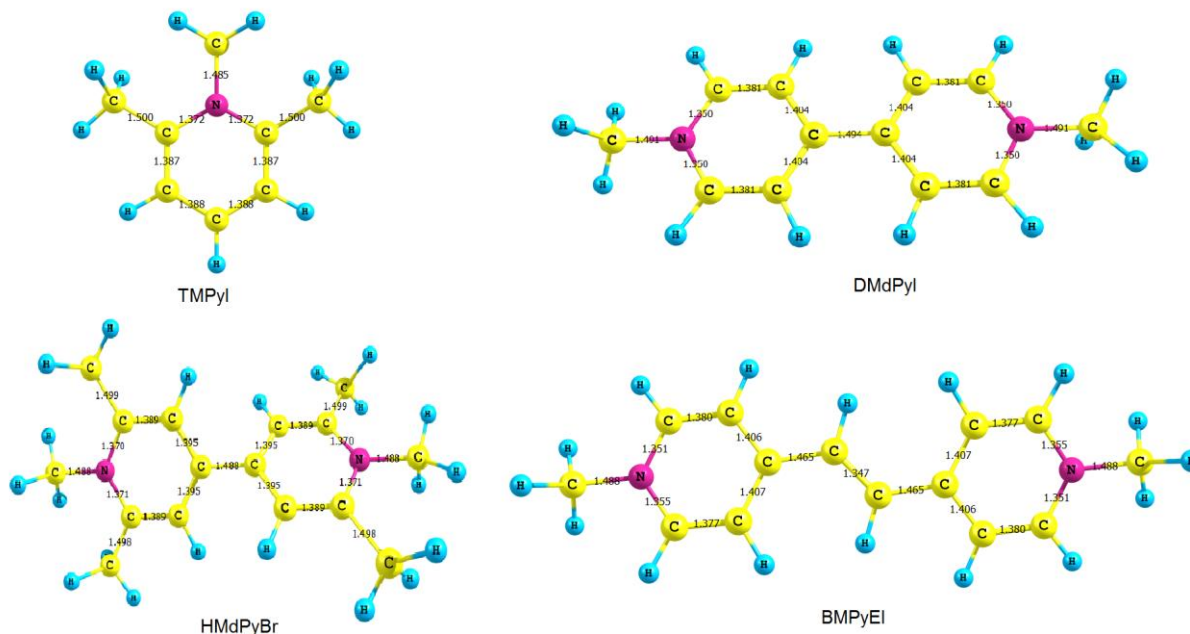
Table 5. Thermodynamic parameters of the studies inhibitors on Al in 1 M HCl

Inhibitor	E <sub>a</sub> <sup>o</sup> (kJ mol <sup>-1</sup> )	ΔH <sup>o</sup> (kJ mol <sup>-1</sup> )
Pure		26.6
TMPyI	19.98	15.78
DMdPyI	19.87	24.0
HMdPyBr	17.25	27.3
BMPyEI	11.25	32.5

### 3.5. Molecular orbital calculations

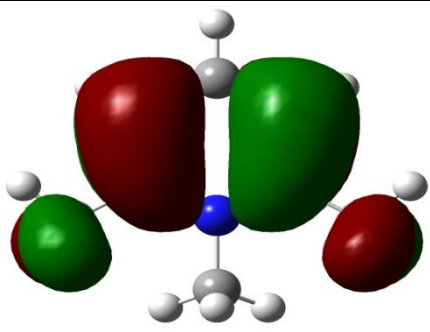
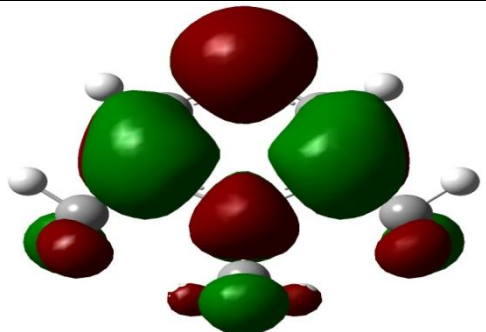
We employed DFT/B3LYP/6-311+G\*\* level of theory to investigate the electronic structure of the studied inhibitor compounds, the optimized geometries and bond distance (Å) are indicated in Fig.8. We have used Frontier Molecular Orbital Theory (FMO) to analyze the chemical reactivity of these compounds. According to the frontier molecular orbital theory, the energy of the highest occupied molecular orbital (E<sub>HOMO</sub>) and lowest unoccupied molecular orbital (E<sub>LUMO</sub>) are important quantum chemical indices for predicting the reactivity of a chemical species. Basically, adsorption on the metal surface and thus the inhibition efficiency of any chemical compound is increased with increasing E<sub>HOMO</sub> values. Previous studies indicated that the ability of adsorption of inhibitors increases with lower E<sub>LUMO</sub> and the energy gap (E<sub>g</sub>=E<sub>LUMO</sub>-E<sub>HOMO</sub>) values[14,15].

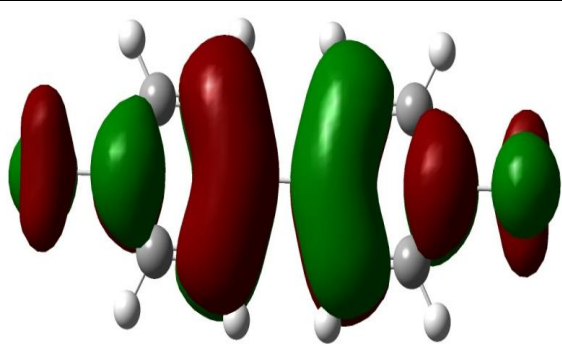
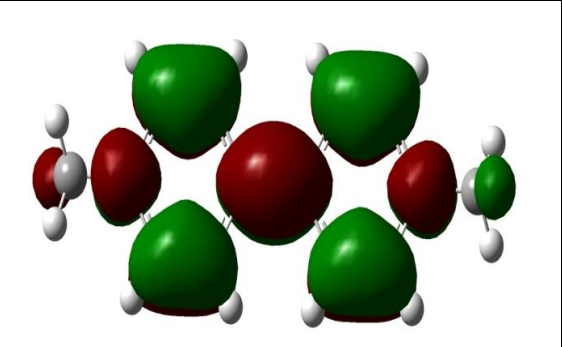
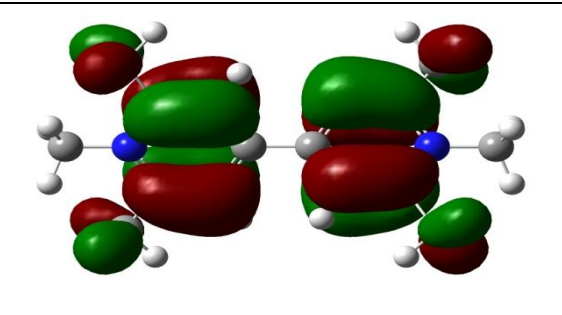
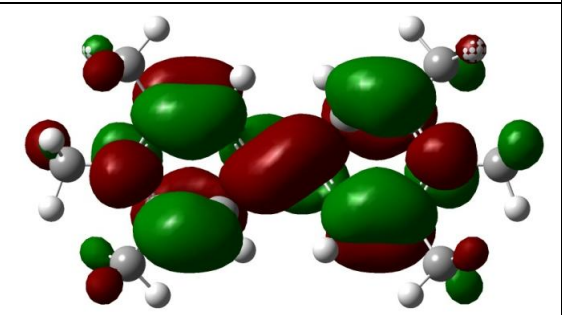
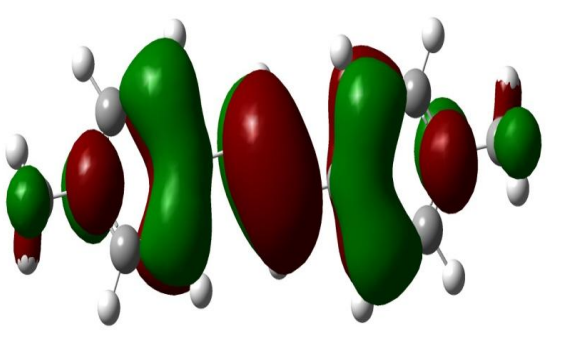
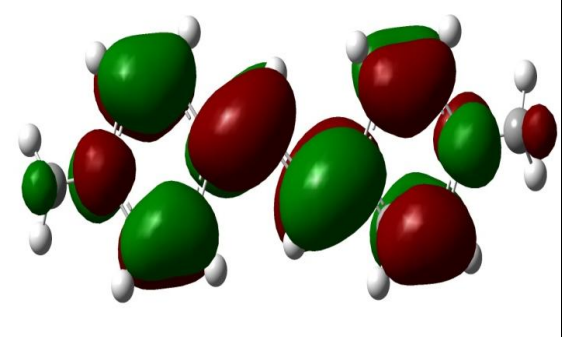
The HOMO, LUMO and frontier orbital energy gap of all the studied compounds calculated from B3LYP/6-311+G\*\* level of theory are given in Table 6. The band gap of compound BMPyEI is less than the other three compound inhibitors and hence, we can conclude that the compound BMPyEI is more reactive than others. The molecular orbitals (HOMO and LUMO) analysis of the present compound shows that the studied compounds are a potential corrosion inhibitor. As display in Table 6, the electron density distribution of HOMO and LUMO orbital delocalize over the structure in all studied compounds. From these results, we suggest that the interaction between the studied bipyridines with Al surface will be physical adsorption.



**Figure 8.** Optimized geometries and bond distance (Å) with B3LYP/6-311+G\*\* for the inhibitor compounds.

**Table 6.** Electron density distribution and energy of the HOMO and LUMO orbitals.

Inhibitor	E <sub>g</sub>	HOMO/au	LUMO/au
TMPyI	0.204	 -0.437	 -0.233

DMdPyI		
	0.181	-0.568
HMdPyBr		
	0.178	-0.526
BMPyEI		
	0.146	-0.508

### 3.6. Mechanism of inhibition

Although the inhibition efficiencies of the studied inhibitors are lower, but they could be valuable inhibition for aluminum which suspected to pitting corrosion due to the high concentration of the studied solution of HCl. In addition, the studied inhibitors showed significant increase in the inhibition action with temperature, few inhibitors could affected in these conditions. The active surface compounds (surfactants) have hydrophilic head and hydrophobic tail, they adsorbed on surfaces through the head, i.e. physical adsorption, and left tail in the solution [22]. The more heads in the molecules meaning more adsorption centers and make the adsorbed molecule more flat on the metal surface. The horizontal position of the benzene ring facilitates the exchange of electrons ( $\pi$  electrons in aromatic ring) with the metal surface, and this process is a chemical adsorption which increases adhesion of molecules. The electrochemical results and isothermal adsorption calculations showed that the bipyridines under study have physical and chemical adsorption on aluminum surface. However, most of electrochemical result and isothermal adsorption calculation showed that the bipyridines under study have strong physical adsorption on aluminum surface. The adsorption of

bipyridinium cations eventually formed an adherent protective layer on the Al surface, strengthening the corrosion inhibition and decreasing the destructive action of chloride ion. In his study, Free [23] relates the surfactant adsorption on a metal surface to corrosion inhibition by stating that inhibition is proportional to effective coverage, rather than actual coverage. The salts of dipyridinium rings showed similar inhibition behavior as that of the mono-pyridinium ring. In addition, the experimental results revealed that all the investigated compounds have equal efficiencies.

#### 4. CONCLUSIONS

- The organic compounds of multiple pyridinium rings with different activation group were prepared and used as inhibitor for aluminum corrosion.
- The bipyridines have inhibition action against the general and pitting corrosion of Al in 1 M HCl solution in range of different temperatures.
- The bipyridines compounds adsorbed physically on the Al surface and their inhibition efficiencies increased with temperature.
- The bipyridines compounds worked as mixed inhibitors with mainly anodic.

#### ACKNOWLEDGMENT

This project was funded by Deanship of Scientific Research (DSR), King Abdulaziz University, Jeddah, under Grant No. 468/130/1432. The authors, therefore, acknowledge with thanks DSR technical and financial support.

#### References

1. T. Haruna, T. Kouno, and S. Fujimoto, *Corros. Sci.*, 47(2005) 2441.
2. E. Hür, G. Bereket, and Y. Şahin, *Curr. Appl. Phys.*, 7(2007) 597.
3. A.M. Abdel-Gaber, B.A. Abd-El-Nabey, I.M. Sidahmed, A.M. El-Zayady, and M. Saadawy, *Mater. Chem. Phys.*, 98(2006) 291.
4. Z. Szklarska-Smialowska, *Corros. Sci.*, 41(1999)1743 .
5. ABDEL, M.T. MAKHLOUF, and A.A.H. MAS, *Br. Corros. J.*, 30(1995)71.
6. A.K. Maayta and N.A.F. Al-Rawashdeh, *Corros. Sci.*, 46(2004) 1129 .
7. V. Karpagam, S. Sathiyarayanan, and G. Venkatachari, *Curr. Appl. Phys.*, 8(2008) 93.
8. X. Mao, X. Liu, and R.W. Revie, *Corrosion*, 50(1994) 651.
9. L. Wang, G.-J. Yin, and J.-G. Yin, *Corros. Sci.*, 43(2001) 1197.
10. S.A.A. El-Maksoud, *J. Electroanal. Chem.*, 565(2004) 321.
11. M.S. Morad, A.A. Hermas, A.Y. Obaid, and A.H. Qusti, *J. Appl. Electrochem.*, 38(2008) 1301.
12. P. Stipa, *Spectrochim. Acta. A. Mol. Biomol. Spectrosc.* 64(2006) 653.
13. A.Y. Obaid, S.A. Al-Thabaiti, A.H. Qusti and A.A. Hermas, *Asian J. Chem.*, 25(2013)3781.
14. F. Bentiss, M. Bouanis, B. Mernari, M. Traisnel, H. Vezin, and M. Lagrenée, *Appl. Surf. Sci.*, 253(2007) 3696 .
15. M.M. El-Naggar, *Corros. Sci.*, 49(2007) 2226 .
16. M. Mahdavian, S. Ashhari, *Electrochim. Acta*, 55 (2010) 1720.
17. L. Vrsalović, S. Gudić, M. Kliškić, E. E. Oguzie, L. Carev, *Int. J. Electrochem. Sci.*, 11 (2016) 459

18. C. Lee, W. Yang, and R.G. Parr, *Phys. Rev.*, 37(1988) 785.
19. S.-Z. Yao, X.-H. Jiang, L.-M. Zhou, Y.-J. Lv, and X.-Q. Hu, *Mater. Chem. Phys.*, 104(2007) 301.
20. R. Agrawal and T.K.G. Nambodhiri, *Corros. Sci.*, 30(1990) 37.
21. X. Li, S. Deng, and H. Fu, *Corros. Sci.*, 53(2011) 2748.
22. R. Zyaaya, J.L. Dawson, *J. Appl. Electrochem.*, 24 (1994) 943.
23. M.L. Free, *Corros. Sci.*, 46(2004) 3101.

© 2016 The Authors. Published by ESG ([www.electrochemsci.org](http://www.electrochemsci.org)). This article is an open access article distributed under the terms and conditions of the Creative Commons Attribution license (<http://creativecommons.org/licenses/by/4.0/>).